

Pion scattering to 4^- states in ^{14}C

D. B. Holtkamp,* S. J. Seestrom-Morris, and D. Dehnhard
University of Minnesota, Minneapolis, Minnesota 55455

H. W. Baer and C. L. Morris
Los Alamos National Laboratory, Los Alamos, New Mexico 87545

S. J. Greene*
New Mexico State University, Las Cruces, New Mexico 88003

C. J. Harvey
University of Texas, Austin, Texas 78712

D. Kurath
Argonne National Laboratory, Argonne, Illinois 60440

J. A. Carr
Florida State University, Tallahassee, Florida 32306
 (Received 3 July 1984)

Angular distributions and excitation functions for inelastic scattering of π^+ and π^- from ^{14}C were measured at incident pion energies near the Δ_{33} resonance. Three states at excitation energies 11.7, 15.2, and 17.3 MeV were identified as 4^- states. Isovector and isoscalar spectroscopic amplitudes Z_0 and Z_1 , and equivalently, neutron and proton amplitudes Z_n and Z_p were deduced by comparison with microscopic distorted wave impulse approximation calculations. The 11.7-MeV state was found to be excited with a Z_n/Z_p amplitude ratio of $-1/3$, resulting in a complete cancellation of the π^+ cross section. A nearly pure proton excitation was observed for the transition to the 17.3-MeV state. Both results are in qualitative agreement with the presented shell-model calculations. A poor correspondence with theory is found for the 15.2-MeV state. Data and distorted-wave impulse approximation calculations using shell-model wave functions are presented for the first 3^- state at 6.73 MeV as an example of a transition dominated by $\Delta S=0$ (no spin transfer). Its excitation function and angular-distribution shape contrast sharply with the transitions to the 4^- states that proceed by $\Delta S=1$.

I. INTRODUCTION

Pion inelastic scattering at energies near the Δ_{33} resonance provides a powerful means for measuring the proton and neutron components in nuclear wave functions. States that are especially well suited for quantitative analysis are the so-called "stretched" one-particle-one-hole (1p-1h) states. For even- A , even- Z nuclei, these are negative-parity states with angular momentum $J=j_p+j_h$, where $j_p=l_p+\frac{1}{2}$ and $j_h=l_h+\frac{1}{2}$ are the total angular momenta of the particle and hole, respectively. Specifically, for ^{14}C these are 4^- states formed by coupling a $1d_{5/2}$ particle to a $1p_{3/2}$ hole. More than for other types of states, the excitation of stretched states in inelastic scattering is expected to correspond to a single p-h excitation built on the ground state. In this approximation a single, isospin-dependent transition density determines the probability of exciting the state by scattering of electrons, protons, or pions.¹⁻³ This simplifies considerably their interpretation, making these transitions good candidates for tests of reaction theories and structure calculations.

The 4^- states have exceptionally clear signatures for identifying them in inelastic pion scattering.^{4,5} Their ex-

citation functions at fixed-momentum transfer q exhibit an approximate $\sin^2\theta$ dependence (where θ is the scattering angle) because of the spin transfer $\Delta S=1$ involved. Other states produced with the same angular-momentum transfer of $\Delta L=3$ but without spin transfer ($\Delta S=0$) have fixed- q excitation functions that follow a $\cos^2\theta$ dependence. The angular-distribution shapes of the two types of $\Delta L=3$ transitions also differ in that the $\Delta S=1$ transitions peak at larger q than $\Delta S=0$ transitions. These signatures are clearly demonstrated in the present study.

In a recent Letter⁶ results from inelastic scattering of 164-MeV pions from ^{14}C were briefly reported. Cross-section ratios were found that could only be explained by an almost complete cancellation of the proton and neutron parts of the transition-density amplitudes for either π^+ or π^- scattering. The angular distributions (not shown in the Letter) for two of the states with large cross-section ratios suggested a spin and parity assignment of $J^\pi=4^-$. These data, the first experimental evidence for $M4$ transitions in ^{14}C , thus promised to give some insight into the distribution of $M4$ strength between neutrons and protons in light $N\neq Z$ nuclei. In this paper we present a full study of the data for pion inelastic scattering to the 4^-

states in ^{14}C .

In Secs. II and III we describe the experiment and present the excitation functions for three states in ^{14}C that appear to be excited predominantly by $\Delta S=1$ transitions. We also show the excitation function for the 3^- state at 6.73 MeV, a collectively enhanced state, which provides a good example of the excitation function of an almost pure $\Delta S=0$ transition. The shapes of the angular distributions and the clear difference between $\Delta S=0$ and 1 excitation functions are used to empirically identify three $M4$ transitions. In Sec. IV we describe the distorted-wave calculations of the pion angular distributions. In Sec. V we describe the technique used to extract the isoscalar and isovector transition-density amplitudes (Z coefficients) for the 4^- states. We make use of the complementary information that the recent electron-scattering data⁷ provide about the $\Delta T=1$ parts of the transition densities for two of the states. In Sec. VI we present distorted wave impulse approximation (DWIA) calculations for the cross sections for the $^{14}\text{C}(p,p')$ reaction based on the spectroscopic amplitudes deduced from our analysis. In Sec. VII we describe new shell-model calculations for these 4^- states and compare the theoretical spectroscopic amplitudes for the $(d_{5/2}, p_{3/2}^-)$ 1p-1h excitation with those deduced from the data. In Secs. VIII and IX we present sum rules for stretched states, discuss the fragmentation of the $M4$ transition strength, suggest possible improvements in the theoretical wave functions, and discuss the evidence for 3p-3h admixtures in the 4^- states given by recent three-particle transfer-reaction data. Our conclusions are presented in Sec. X.

II. EXPERIMENTAL PROCEDURE

The experiment was performed at the Clinton P. Anderson Meson Physics Facility (LAMPF) using the energetic pion channel and spectrometer (EPICS) system described elsewhere.⁸ The beam energy was 164 MeV. The target consisted of ~ 9 g of carbon powder enriched to about 80% in ^{14}C . Details of the target design have been discussed previously,⁶ together with some of the other results of the experiment. Typical π^+ and π^- spectra are shown in Fig. 1. The energy resolution is about 200 keV (FWHM) and the uncertainty in the extracted excitation energies is about 100 keV.

The ^{14}C cross sections were normalized to the π^\pm cross sections for the 4.44-MeV state in ^{12}C , using the ^{12}C (4.44 MeV) yield from the ^{14}C target and the measured $^{14}\text{C}/^{12}\text{C}$ atom ratio, r . We chose this method of normalization because it does not rely on the assumption of uniform target thickness. The atom ratio was determined from five target assays done at Oak Ridge National Laboratory. The average of these measurements is $r=4.6\pm 0.4$, where the error represents the rms deviation in the five measurements. The cross sections presented in Ref. 6 were based on the first target assay, which had yielded $r=4.87\pm 0.24$. Also, we found that in our first analysis⁶ the peak area for the 4.44-MeV state in ^{12}C , which was used to normalize the ^{14}C cross sections, contained some background from the stainless steel frame. Correcting for this and using the new value of r yields the peak cross sections listed in

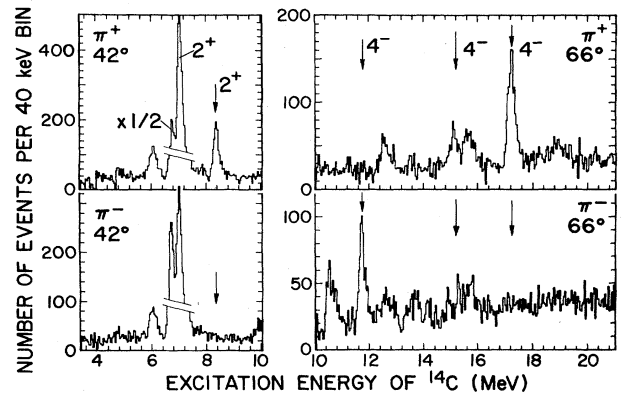


FIG. 1. Spectra from inelastic scattering of π^+ and π^- on ^{14}C . The 4^- states at 11.7, 15.2, and 17.3 MeV are identified by arrows in the 66° spectra.

Table I. These are a factor of 1.25 larger than reported in Ref. 6. The new normalizations result in elastic-scattering cross sections in excellent agreement with optical-model calculations.¹⁰ The large uncertainty in the atom ratio (10%), added in quadrature to the 10% error in absolute cross-section scale, results in an overall uncertainty in the absolute normalization of $\pm 14\%$. The errors shown in the figures are due only to statistical errors and uncertainties in the peak fitting; they do not include the overall normalization error of $\pm 14\%$. Also shown in Table I are the measured excitation energies and the cross-section ratios $R = \sigma(\pi^+)/\sigma(\pi^-)$.

III. EXPERIMENTAL RESULTS

A. Identification of $M4$ transitions

Sections of π^+ and π^- spectra measured at $\theta_{\text{lab}}=42^\circ$ and 66° are shown in Fig. 1. The peaks observed at 66° , where the momentum transfer q is approximately 1.5 fm^{-1} , are due to high-spin states and the remnants of strong low-spin states that peak at lower q . Angular distributions for three peaks, at 11.7, 15.2, and 17.3 MeV, are shown in Fig. 2. These have maxima near $\theta_{\text{c.m.}}=65^\circ$ and are similar in shape to those observed for known $M4$ transitions in ^{12}C (Ref. 11), ^{13}C (Refs. 12 and 13), and ^{16}O (Ref. 14). Based on this similarity, these states had been tentatively identified⁶ as 4^- states. Results for the first and second excited 2^+ states at 7.01 and 8.32 MeV (see the left-hand side of Fig. 1) have been presented in Refs. 6 and 15.

Excitation functions measured at fixed-momentum transfer $q=1.45 \text{ fm}^{-1}$, corresponding to the peaks of the measured angular distributions, are shown in Fig. 3. It was shown by Siciliano and Walker⁵ that the constant- q cross sections for $\Delta S=1$ transitions should decrease as $\sin^2\theta$ with increasing energy (long-dashed line in Fig. 3). (Note that for the excitation-function measurement, θ is decreased as the incident energy is increased to keep q constant.) In contrast, excitation functions for $\Delta S=0$ transitions increase according to $\cos^2\theta$. Such differing excitation functions have been observed⁴ for transitions in

TABLE I. Experimental and theoretical peak cross sections and deduced spectroscopic amplitudes for the observed 4^- states in ^{14}C .

J^π	E_x (MeV)	Experiment		R^b	DWIA calculations		Deduced spectroscopic amplitudes ^a	
		$\sigma_{\text{pk}}(\pi^+)$ ($\mu\text{b}/\text{sr}$)	$\sigma_{\text{pk}}(\pi^-)$ ($\mu\text{b}/\text{sr}$)		$\sigma_{\text{pk}}(\pi^+)^c$ ($\mu\text{b}/\text{sr}$)	$\sigma_{\text{pk}}(\pi^-)^c$ ($\mu\text{b}/\text{sr}$)	Z_0	Z_1
4^-	11.7 ± 0.1	< 4	67 ± 4	$< \frac{1}{17}$	0.1	69	-0.18 ± 0.04	-0.33 ± 0.01
4^-	15.2 ± 0.1	33 ± 4	17 ± 5	1.9 ± 0.6	34	19	0.22 ± 0.06	-0.05 ± 0.03
4^-	17.3 ± 0.1	110 ± 8	< 10	> 11	111	10	-0.26 ± 0.03	0.27 ± 0.01
3^-	6.7 ± 0.1	490 ± 50	1010 ± 80	2.1 ± 0.3	201	624		

^aIsoscalar (Z_0) and isovector (Z_1) transition-density amplitudes (as defined in Ref. 9) for the $(1d_{5/2}, 1p_{3/2}^{-1})$ 4^- particle-hole excitation. Errors in extracting the values from the data are discussed in Sec. V.

^b $R \equiv \sigma_{\text{pk}}(\pi^+)/\sigma_{\text{pk}}(\pi^-)$.

^cFor the 4^- states, these are the peak cross sections given by the DWIA calculations (renormalized by the factor 1.8) using the Z_0 and Z_1 values given in the last two columns. The harmonic-oscillator size parameter $\alpha = (M\omega/\hbar)^{1/2}$ is 0.649 fm. For the 3^- state the values correspond to the shell-model calculations of Sec. VI and the use of Eq. (13).

^{13}C . Clearly, the excitation functions for the three proposed 4^- states decrease with increasing energy, following approximately the $\sin^2\theta$ behavior. This result supports the 4^- assignment, since the stretched $(d_{5/2}, p_{3/2}^{-1})$ 4^- configuration can be reached only by a $\Delta L=3$, $\Delta S=1$ transition.

To demonstrate the reliability of the method of discriminating between $\Delta S=1$ and 0 transitions by measurement of fixed- q excitation functions, data for the transition to the low-lying 3^- state at 6.73 MeV in ^{14}C are shown in Figs. 4 and 5. This collective octupole transition is expected to be dominated by $\Delta S=0$ components (Sec. VIII). One sees from Fig. 4 that the angular-distribution shape for this $\Delta L=3$, $\Delta S=0$ transition differs from the $\Delta L=3$, $\Delta S=1$ shapes for the 4^- states (Fig. 2) in that the maximum is at a smaller angle ($\sim 42^\circ$) and that the angular width of the diffraction peak is narrower. For the 3^- state, the constant- q excitation function (Fig. 5) was measured at $q \simeq 0.96 \text{ fm}^{-1}$, corresponding to the peak of the angular distribution. Indeed, the excitation functions for π^+ and π^- scattering to the 3^- state increase rapidly with energy in qualitative agreement with the $\cos^2\theta$ behavior for a $\Delta S=0$ transition and in sharp contrast to the decrease in cross section observed for the 4^- candidates.

B. The 2^- , 4^- complex near 24.5 MeV

To search for possible 4^- states in the 20–30-MeV excitation region, we measured a π^+ spectrum at 164 MeV and $\theta_{\text{lab}}=60^\circ$ with this region centered on the focal plane (Fig. 6). A broad structure centered near 24.5 MeV and having a width of ~ 1.7 MeV is evident. There is also an indication that this structure includes a narrower peak at 24.4 MeV. In a subsequent $^{14}\text{C}(e,e')$ experiment⁷ at 180° , a 4^- state was identified at 24.3 MeV having a width $\Gamma(\text{FWHM}) < 0.3$ MeV and a peak cross section comparable to the 4^- states at 11.7 and 17.3 MeV. This raised the question as to why it was not as clearly observed in the π^+ spectrum. Since the 4^- state at 24.3 MeV is believed⁷ to be a $T=2$ state, its excitation must be purely isovector and it would have nearly equal π^+ and π^- cross

sections. Furthermore, its absolute cross section would be only 0.25 of that of a purely isoscalar transition of the same spectroscopic amplitude (Z coefficient). One can estimate its peak cross section relative to the 17.3-MeV state using the $(d_{5/2}, p_{3/2}^{-1})$ spectroscopic amplitudes given in Sec. IV and Ref. 7, and the relation

$$\frac{\sigma(\pi^+; 4^-, T=2, 24.3)}{\sigma(\pi^+; 4^-, T=1, 17.3)} = \left[\frac{Z_1(24.3)}{2Z_0(17.3) - Z_1(17.3)} \right]^2, \quad (1)$$

which follows from the analysis presented in Sec. V. Inserting the value $Z_1(24.3)=0.40$ (Ref. 7) and the values $Z_0(17.3)=-0.26$ and $Z_1(17.3)=0.27$ given in Table I, gives $\sigma(24.3)/\sigma(17.3)=0.26$. The areas of the 17.3-MeV state and the broad complex centered near 24.5 MeV as shown in the spectrum of Fig. 6 are equal to within 10%. It is completely consistent with the π^+ spectrum to have 25% of the 24.5-MeV complex be due to a relatively narrow state at 24.3 MeV. Indeed, as already mentioned, there is the suggestion of such a peak in the spectrum. One cannot, however, obtain a reliable cross section for this state from the π^+ data because it cannot be unambiguously separated from the other states in the 23.7–25.4-MeV region.

Some information on this excitation region is available from other experiments. In the $^{14}\text{C}(\pi^-, \gamma)^{14}\text{B}$ reaction with stopped pions, a broadened 2^- state at 2.1-MeV excitation in ^{14}B was observed.¹⁶ The analog of this $T=2$ state would occur at approximately 24.3 MeV in ^{14}C . The low- q data⁷ on the $^{14}\text{C}(e,e')$ reaction at 180° also show a broad structure at 24.3 MeV having a width $\Gamma \simeq 0.9$ MeV (FWHM). Thus one candidate for an interfering state is a 2^- , $T=2$ state with an excitation energy within 0.1 MeV of the 4^- state. It appears that there may be more states near 25-MeV excitation contributing to the π^+ cross section at 60° , because a 2^- state at 24.3 MeV having a width of 0.9 MeV could not produce the large π^+ yield observed at 25.0 MeV (Fig. 6). Candidates for additional states are given by the shell-model calculations discussed in Sec. VI, which predict several 4^- , $T=1$ states near 25 MeV. Calculated 4^- states at 24.2 and 24.6 MeV have predicted π^+ peak cross sections of 0.09 and 0.03 mb/sr, respectively,

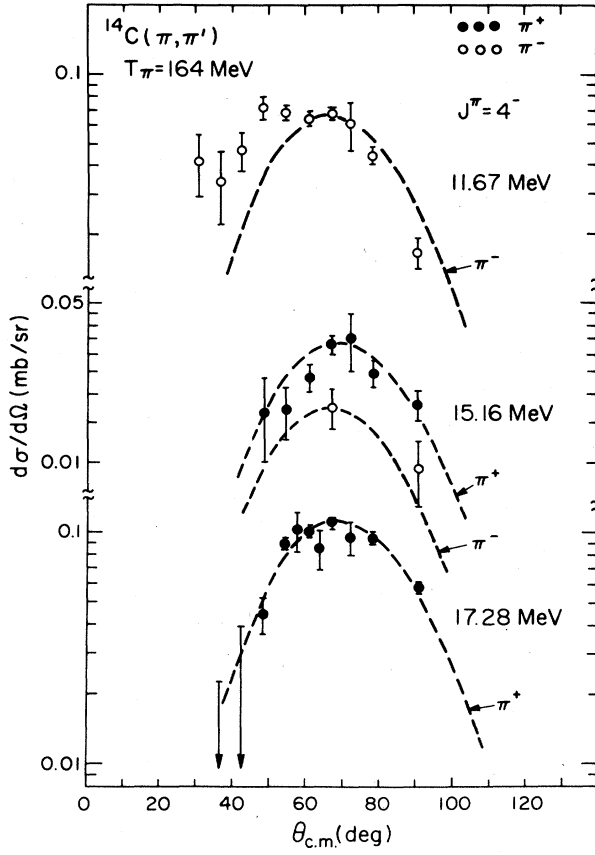


FIG. 2. Experimental and theoretical angular distributions for the 4^- states. The DWIA calculations were done assuming a pure $(d_{5/2}, p_{3/2})$ particle-hole excitation.

compared to 0.04 mb/sr predicted for the 4^- , $T=2$ state calculated to be at 24.4 MeV. The $B(M4)$ values for these $T=1$ states are small, and thus the calculated cross sections for 180° electron scattering are very small relative to the $T=2$ state. Thus the presence of 4^- states with predominant isoscalar-transition amplitudes would be consistent with the present experimental situation.

IV. DISTORTED-WAVE CALCULATIONS

The distorted-wave calculations were made using a simple single-scattering model for pion-induced unnatural-parity transitions in nuclei. A recent paper¹⁷ describes this model and calibrates it by comparison to data^{14,18} for the 4^- states in ^{16}O and 6^- states in ^{28}Si . For completeness we give a general description of the model here.

The spin-dependent part $t_{\pi N}^{LS}$ of the pion-nucleon interaction is given in momentum space by

$$t_{\pi N}^{LS} = -i(t_0^{LS} + t_1^{LS} \mathbf{t}_\pi \cdot \boldsymbol{\tau}_N) \boldsymbol{\sigma}_N \cdot \mathbf{k} \times \mathbf{k}' \quad (2)$$

in the pion-nucleon center-of-mass (c.m.) frame, where $\boldsymbol{\sigma}_N$ is the nucleon Pauli-spin operator, \mathbf{t}_π is the pion-isospin operator, and $\boldsymbol{\tau}_N$ is twice the nucleon-isospin operator. The impulse approximation¹⁹ estimates for the isoscalar (t_0^{LS}) and isovector (t_1^{LS}) parts of $t_{\pi N}^{LS}$ are obtained using the phase shifts of Ref. 20. The nuclear matrix element

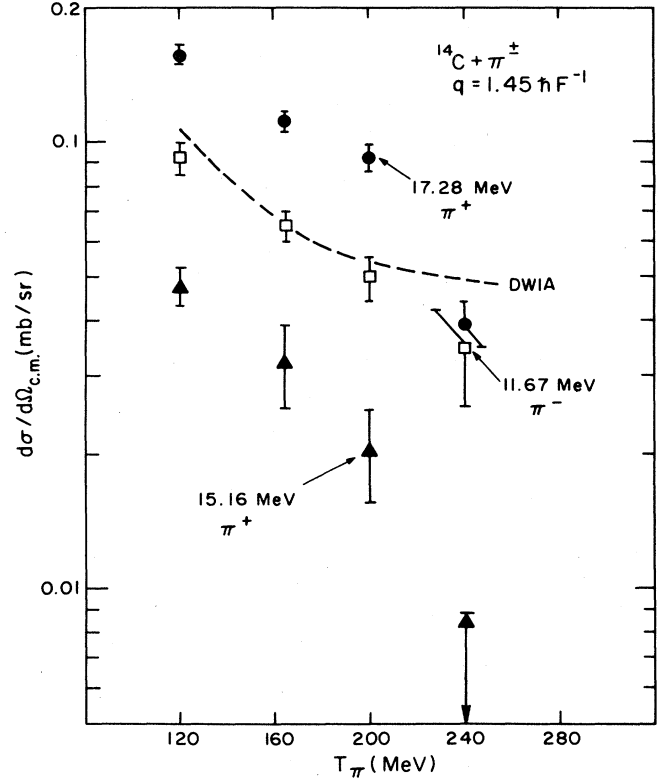


FIG. 3. Experimental fixed- q excitation functions for the 4^- states. DWIA calculations are shown for the 11.7-MeV state.

of $t_{\pi N}^{LS}$ gives the scattering potential $U_{\pi A}$, which can be written as

$$U_{\pi A} = \bar{U}_J(r_\pi) [Y_J(\hat{r}_\pi) \times \nabla_\pi]^J, \quad (3)$$

where

$$\bar{U}_J(r_\pi) = \gamma \alpha_\pi \frac{2}{\pi} \sum_{n,T} k_n^2 \Delta k_n j_J(k_n r_\pi) \epsilon^T t_T^{LS} k_n^2 \rho_{JT}^{s\perp}(k_n) \quad (4)$$

is essentially the form factor required for the distorted-wave calculation. It is evaluated using the discretized momentum technique²¹ with $k_n = n(\pi/R)$, $R=12$ fm, and $n=1,2,\dots,40$. Here $\gamma \approx k\omega_c/k_c\omega$ and $\alpha_\pi \approx k_c/k$ are factors required by the transformation from the pion-nucleon to the pion-nucleus c.m. system,²² k and ω (k_c and ω_c) are the pion momentum and total energy in the pion-nucleus (pion-nucleon) center of mass, and ϵ^T is 1 for $T=0$ and ∓ 1 for $T=1$ for π^\pm scattering. The transverse spin-transition density $\rho_{JT}^{s\perp}(k_n)$ that appears in Eq. (4) is defined by

$$\rho_{JT}^{s\perp}(k_n) = \left[\frac{J+1}{2J+1} \right]^{1/2} \rho_{J,J-1}^{sT}(k_n) - \left[\frac{J}{2J+1} \right]^{1/2} \rho_{J,J+1}^{sT}(k_n), \quad (5)$$

where

$$\rho_{J,L}^{sT}(k_n) = \left\langle f \left| \sum_N j_L(k_n r_N) [Y_L(\hat{r}_N) \times \boldsymbol{\sigma}_N]^J \boldsymbol{\tau}_N^T \right| i \right\rangle. \quad (6)$$

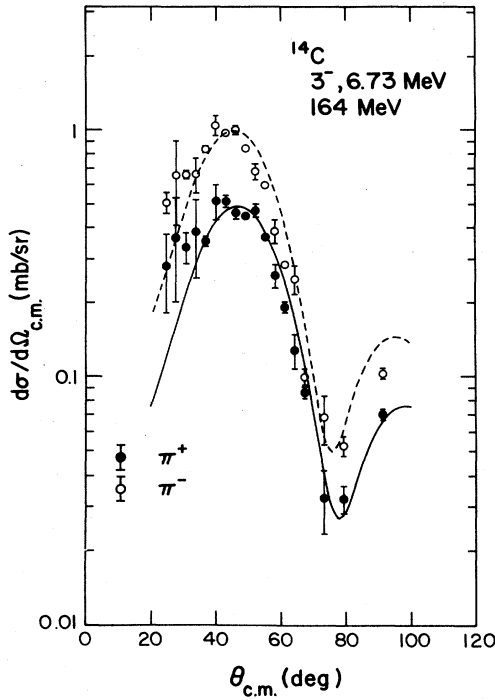


FIG. 4. Angular distributions for π^+ and π^- scattering to the 3^- state at 6.73 MeV in ^{14}C . The DWIA calculations were done using the shell-model wave functions and an isoscalar-enhancement factor of 1.5, as discussed in Sec. VII.

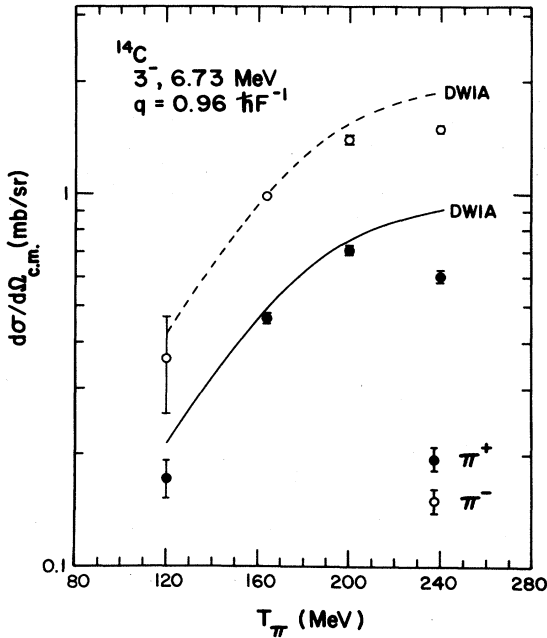


FIG. 5. Fixed- q excitation functions for the 3^- state. The DWIA calculations are based on the shell-model wave functions and an isoscalar-enhancement factor of 1.5, as discussed in Sec. VII.

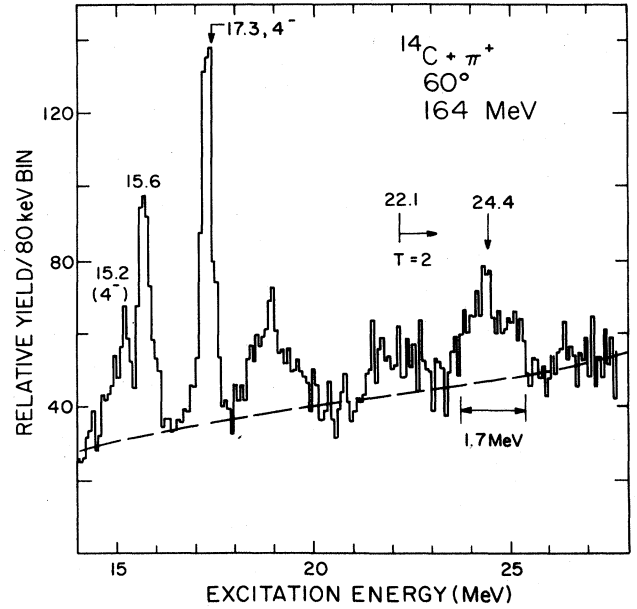


FIG. 6. The π^+ spectrum with the higher excitation region centered on the focal plane. There is a suggestion of a peak at 24.4-MeV excitation, which is close in energy to the known (Ref. 7) 4^- , $T=2$ state at 24.3 MeV. Other states in this energy region are also excited, as discussed in the text.

Note that $\rho_{J,J+1}^{sT}$ vanishes for stretched configurations. Since the current transition densities also vanish^{1-3,5} in this special case, the single isospin-dependent density required for the pion-scattering calculations is also the only transition density needed to calculate the cross sections for (e,e') and (p,p') reactions. The direct relationship between various reactions that excite a stretched state makes interpretation of the data more straightforward than is usual. It should be noted that this is strictly true only if we assume that proton and neutron wave functions have the same radial dependence and that only $1\hbar\omega$ excitations are allowed.

The scattering potential in Eq. (4) was generated by the code ALLWRLD (Ref. 23) and used in the code MSUDWPI (Ref. 24) to calculate the distorted-wave-approximation angular distributions for the 4^- states. Similar approaches have been followed by Siciliano and Walker,⁵ who use the eikonal model for the distorted waves, and Lee and Kurath,²⁵ who use a nonlocal pion-nucleon t matrix and execute the full calculation in momentum space. These different approaches give similar relative cross sections for states of a given J^π , but usually require somewhat different overall normalizations. Predictions of the model given by Eq. (4) are compared to that of Lee and Kurath in Sec. VII.

V. EXTRACTION OF THE SPECTROSCOPIC AMPLITUDES Z_0 AND Z_1

The determination of spectroscopic amplitudes for the 4^- states reported here was made considerably more pre-

cise by the recent electron-scattering measurements⁷ of the transverse magnetic form factor of the 11.7- and 17.3-MeV states, which allowed us to fix the average radial dependence of $\rho_{J,T-1}^{ST}$. Assuming a $(d_{5/2}, p_{3/2}^{-1})$ 4^- harmonic-oscillator model for the transition density, these data determine the oscillator-size parameter $\alpha = (M\omega/\hbar)^{1/2}$ to be 0.649 fm^{-1} , where the usual finite size and center-of-mass corrections²⁶ are made. (The center-of-mass corrections to the shell-model wave functions were made in a consistent fashion for the pion-scattering calculations.) Since magnetically scattered electrons see $\Delta T = 1/\Delta T = 0$ in the cross-section ratio 29 to 1, these data are mainly sensitive to the magnitude of the $\Delta T = 1$ transition density. In contrast, π^\pm scattered at energies near the Δ_{33} resonance see $\Delta T = 1/\Delta T = 0$ in the cross-section ratio 1 to 4. Thus the pion cross sections are well suited for determining the $\Delta T = 0$ transition density.

The extraction of Z_0 and Z_1 for mixed isoscalar-isovector transitions is greatly facilitated by the use of closed-form expressions, which for the stretched states approximate closely the results of DWIA calculations. These formulae exhibit explicitly the Z_0, Z_1 correlations in the measurements and provide a means for evaluating the errors in the extracted values.

The measured 180° electron-scattering cross sections σ_{exp} at the peak of the form factors were given⁷ in terms of single-particle units $\sigma_{\text{exp}}/\sigma_{\text{sp}}$, which are related to Z_1 and Z_0 by

$$\frac{\sigma_{\text{exp}}}{\sigma_{\text{sp}}} = Z_1^2 (1.87)(1 - 0.187\alpha)^2, \quad (7)$$

where $\alpha = Z_0/Z_1$. The magnetic-moment factor

$$(\mu_p + \mu_n)/(\mu_p - \mu_n) = 0.88/4.706 = 0.187$$

gives the relative weighting of the isoscalar and isovector coupling constants, whereas $\sigma_{\text{sp}} = \sigma_{\text{sp}}(T=1)$ is the "single-particle" cross section defined in Ref. 7. This is the *sum* of the calculated peak cross section for a $(d_{5/2}, p_{3/2}^{-1})$ isoscalar excitation of a $4^- T=0$ state with a spectroscopic amplitude $Z_0=1$ and *one-half* of the calculated peak cross section for a $(d_{5/2}, p_{3/2}^{-1})$ isovector excitation of a $4^- T=1$ state with a spectroscopic amplitude $Z_1=1$.

The pion differential cross sections at the peaks of the angular distribution may be expressed as

$$\sigma_{\text{pk}}(\pi^+) = (aZ_0 - Z_1)^2 N^+ \sigma_{\text{DW}}^+ \quad (8)$$

and

$$\sigma_{\text{pk}}(\pi^-) = (aZ_0 + Z_1)^2 N^- \sigma_{\text{DW}}^-, \quad (9)$$

where σ_{DW}^\pm are the peak differential cross sections for π^+/π^- scattering given by the DWIA calculations for $(d_{5/2}, p_{3/2}^{-1})$ isovector excitations coupled to $4^-, T=1$. The letter a represents the force ratio t_0^{LS} divided by t_1^{LS} . At 164 MeV, the value $a=1.93$ is obtained from the phase shifts of Rowe *et al.*,²⁰ and it is the value used here for the 4^- states. The N^+ and N^- are renormalization factors for the DWIA calculations to be determined empirically. In a previous study¹⁷ on ^{16}O and ^{28}Si , N^+ and N^- were found equal to within a few percent. We

assume $N^+ = N^- = N$. The DWIA calculations for the ^{14}C 4^- states gave larger peak cross sections for π^+ than for π^- . At the maxima of the angular distributions (68°) we obtained $\sigma_{\text{DW}}^+/\sigma_{\text{DW}}^- \equiv N_D = 1.11$.

The π^+/π^- ratio of measured peak cross sections is, to a first approximation, independent of the DWIA renormalization factor N . It is directly sensitive to the isoscalar-isovector amplitude ratio α in a mixed transition. Using Eqs. (8) or (9) we obtain

$$R \equiv \frac{\sigma_{\text{pk}}(\pi^+)}{\sigma_{\text{pk}}(\pi^-)} = N_D \frac{(a\alpha - 1)^2}{(a\alpha + 1)^2}. \quad (10)$$

This equation can be used to determine α when R is measured, or to restrict the range of α when limits on R are given by the pion data. It is convenient to express the solutions of Eq. (10) in terms of the distortion-corrected ratio $R_c = R/N_D$ and the ratio $2/a$ so that the approximations $a=2$, from the Δ -dominance assumption, and $N_D=1$, from ignoring the charge dependence of the distorted waves, are easily recovered. The two solutions are

$$\alpha_1 = -\frac{(R_c + 1) + 2\sqrt{R_c}}{2(R_c - 1)} \frac{2}{a}, \quad (11a)$$

$$\alpha_2 = -\frac{(R_c + 1) - 2\sqrt{R_c}}{2(R_c - 1)} \frac{2}{a}. \quad (11b)$$

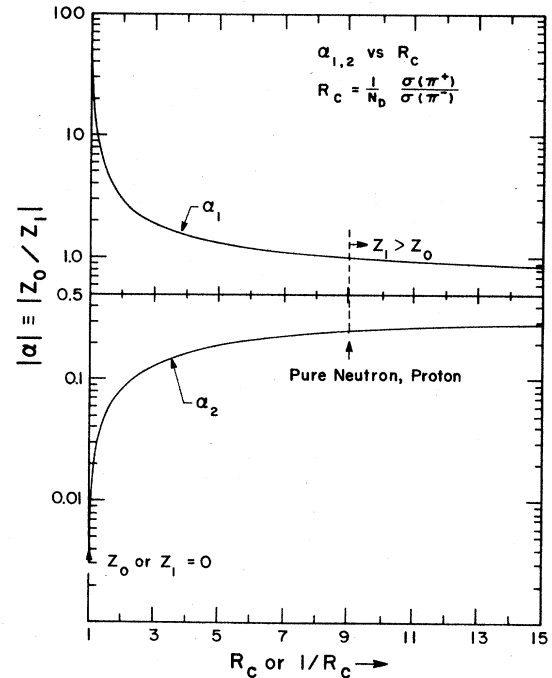


FIG. 7. The two solutions for $\alpha = Z_0/Z_1$ allowed by a measured ratio $R = \sigma_{\text{pk}}(\pi^+)/\sigma_{\text{pk}}(\pi^-)$ of peak pion cross sections. R_c is the distortion-corrected ratio R/N_D , where $N_D = \sigma_{\text{DW}}^+/\sigma_{\text{DW}}^-$ is a correction for the differences in π^+ and π^- distortions (see the text). For $R_c > 1$, α_1 and α_2 are negative; for $R_c < 1$, α_1 and α_2 are positive.

Graphical representations of α_1 and α_2 vs R_c (or $1/R_c$) for $a=2$ are given in Fig. 7. The solutions have the property $\alpha_i(R_c) = -\alpha_i(1/R_c)$, $i=1,2$. Thus if there are two states in the spectrum, one with measured R and the other with a measured $1/R$, the Z_0 and Z_1 for the two states differ only in their relative sign. For $R_c > 1$, both α_1 and α_2 are negative (Z_0 has opposite sign to Z_1) and for $R_c < 1$ the α_i are positive. For $R_c=1$, either Z_0 or Z_1 must be 0; that is, the transition is either purely isovector or purely isoscalar. A third property of the two solutions is that $\alpha_1\alpha_2 = a^{-2}$. An interesting special case occurs when $\alpha_1 = \alpha_2$: the solutions for $R_c = \infty$ are $\alpha_1 = \alpha_2 = -a^{-1}$, whereas for $1/R_c = \infty$ ($R_c = 0$) the solutions are $\alpha_1 = \alpha_2 = a^{-1}$. The preceding discussion also applies to a quantitative study of inelastic proton and neutron scattering to stretched states, provided the value of a is suitably modified.

The combination of pion data and electron-scattering data can provide a precise determination of both Z_0 and Z_1 . In general, the error in Z_1 depends primarily on the error in σ_{exp} of Eq. (7). The error in Z_0 depends primarily on the error in R_c when a definite value of R is measured; when only limits on R are measured, the accuracy to which the normalization factors N^\pm in Eqs. (8) and (9) can be determined is the limiting factor. Since only limits on R could be measured for the 11.7- and 17.3-MeV states in ^{14}C , knowledge of N is essential. The data on the 17.3-MeV state provide a lower limit on N , so we discuss them first.

17.3-MeV state. The measurement $R > 11$ ($R_c > 9.9$) shows that Z_0 and Z_1 have opposite signs. The allowed ranges on α , as calculated from Eq. (11) or read from Fig. 7, are $-\alpha_1 = 0.27$ to 0.52 and $-\alpha_2 = 0.52$ to 1.01 . Using the electron-scattering cross section⁷ $\sigma_{\text{exp}}/\sigma_{\text{sp}} = 0.19 \pm 0.01$ (corrected for meson-exchange currents) together with Eq. (7), we see that restricting α from -0.27 to -1.01 restricts $|Z_1|$ to the range 0.27 – 0.30 . The acceptable ranges of α can be reduced further using Eq. (8) and the measured π^+ peak cross section $\sigma_{\text{pk}}(\pi^+) = 110 \pm 8 \mu\text{b/sr}$, $\sigma_{\text{DW}}^+ = 88.5 \mu\text{b/sr}$, and the condition $\alpha > -1.01$. The relation between $|Z_1|$ and α given by Eq. (8) is shown graphically in Fig. 8(a) for various values of N . One sees that for $|Z_1| < 0.30$ and $\alpha > -1.01$, N must be greater than 1.5. For the range $N=1.5$ to 2.1 , the values of α allowed by the condition $|Z_1| < 0.30$ are -1.01 to -0.8 . Solution α_1 is thereby ruled out for reasonable choices for N .^{17,27} Using Eq. (7), we get $Z_1 = 0.268$ for $\alpha = -1.01$ and $Z_1 = 0.277$ for $\alpha = -0.8$. Thus we obtain $Z_1 = 0.273 \pm 0.015$, where the error arises from the uncertainties in α and in the measured $\sigma_{\text{exp}}/\sigma_{\text{sp}}$.

To determine Z_0 we must specify N . The pion data on the 4^- states in ^{14}C do not provide a sufficiently restrictive upper bound on N . In previous studies the value $N=1.3$ was obtained¹⁷ for ^{16}O and $N=1.5$ – 2.0 was obtained for ^{14}N .²⁷ Since we know from the preceding analysis of the 17.3-MeV state $N \geq 1.5$, we take $N=1.8$ as the most probable value for ^{14}C and assign an error ± 0.3 . This uncertainty includes the normalization error in the data in addition to the systematic errors of our model.

The upper bound $N \leq 2.1$, together with the measured value $|Z_1| = 0.273 \pm 0.015$, restricts α to < -0.92 . The

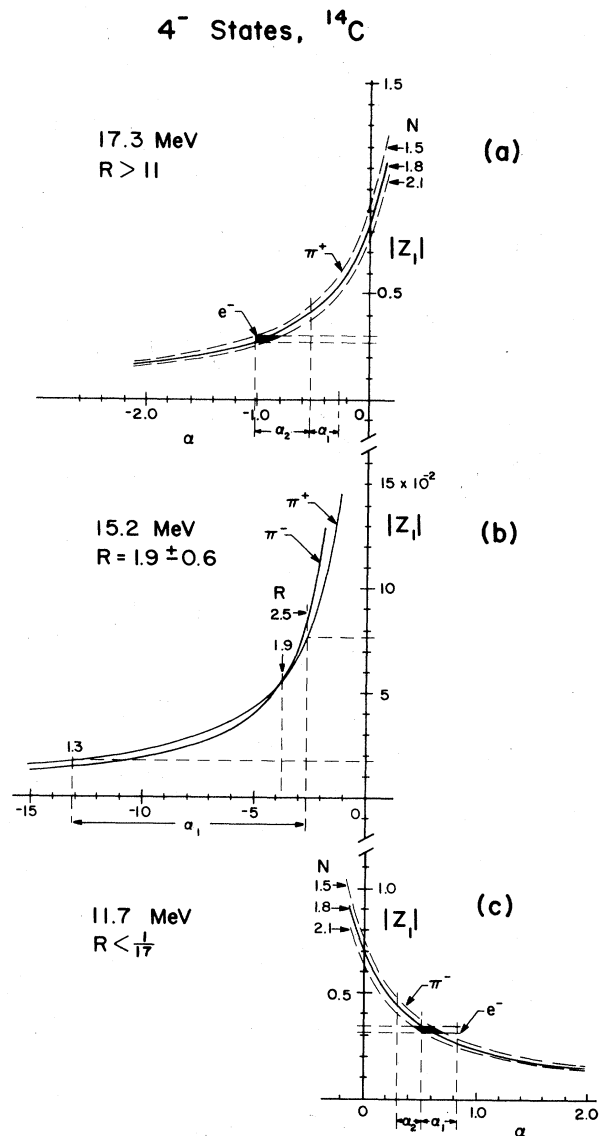


FIG. 8. The loci of $(|Z_1|, \alpha)$ values allowed by the measured π^+ and/or π^- peak cross sections for the 4^- states. The band of $|Z_1|$ values allowed by the 180° electron-scattering cross sections of Ref. 7 are shown for the 17.3- and 11.7-MeV states.

measurement $R > 11$ restricts α to > -1.01 . Thus $Z_0 (= \alpha |Z_1|)$ may vary from -0.291 to -0.237 . Since any value in this interval is equally probable, we obtain the final value $Z_0 = -(0.26 \pm 0.03)$. We have arbitrarily chosen Z_1 to be positive.

11.7-MeV state. The measurement $R^{-1} > 17$ ($R_c^{-1} > 18.9$) shows that Z_0 and Z_1 have the same sign, and it restricts α to values $\alpha_1 = 0.83$ to 0.52 and $\alpha_2 = 0.32$ to 0.52 . Using the electron-scattering results $\sigma_{\text{exp}}/\sigma_{\text{sp}} = 0.16 \pm 0.01$ with Eq. (7) and this range of α , we can restrict $|Z_1|$ to the range 0.311 – 0.345 . The acceptable range on α is further narrowed using the measured $\sigma_{\text{pk}}(\pi^-) = 67 \pm 4 \mu\text{b/sr}$ and the calculated $\sigma_{\text{DW}}^- = 79.7$

$\mu\text{b/sr}$ and Eq. (9). The Z_1 , α , and N correlation for this state is shown in Fig. 8(c). The conditions $1.5 \leq N \leq 2.1$ and $0.311 \leq |Z_1| \leq 0.345$ provide the restriction $0.44 \leq \alpha \leq 0.74$. With this further restriction on α , we obtain $Z_1 = 0.33 \pm 0.01$ by use of Eq. (7).

To determine Z_0 and its error we use Eq. (9) in the form

$$Z_0 = \frac{1}{a} \left\{ -Z_1 \pm \left[\frac{\sigma(\pi^-)}{N\sigma_{\text{DW}}} \right]^{1/2} \right\}. \quad (12a)$$

Since Z_0 and Z_1 must have the same sign, we require the minus sign for the second term on the right-hand side of this equation. Using the values $Z_1 = 0.33 \pm 0.01$, $\sigma_{\text{pk}}(\pi^-) = 67 \pm 4 \mu\text{b/sr}$, $N = 1.8 \pm 0.3$, $a = 1.93$, and $\sigma_{\text{DW}} = 79.7 \mu\text{b/sr}$, we obtain $Z_0 = 0.18 \pm 0.04$. In computing the error, we assumed that the errors in Z_1 , $\sigma(\pi^-)$, and N are independent. The determined Z_0 to Z_1 ratio is $\alpha = 0.55 \pm 0.12$. For $\alpha = 0.55$, we get using Eq. (10) $R_c^{-1} = 490$; for $\alpha = 0.67$, we get $R_c^{-1} = 48$. Thus we see that the expected $\sigma_{\text{pk}}(\pi^+)$ is exceedingly small ($\lesssim 1 \mu\text{b/sr}$) due to the fact that $Z_0 \approx \frac{1}{2} Z_1$ for this state.

15.2-MeV state. The pion data on this state, $\sigma_{\text{pk}}(\pi^+) = 33 \pm 4 \mu\text{b/sr}$ and $\sigma_{\text{pk}}(\pi^-) = 17 \pm 5 \mu\text{b/sr}$, give a definite ratio $R = 1.9 \pm 0.6$ ($R_c = 1.72 \pm 0.55$). Since $R_c > 1$, we know Z_0 and Z_1 to have opposite sign. Also, since the state was not observed in 180° electron scattering, it may be presumed to be predominantly an isoscalar excitation. Use of Eq. (11) or inspection of Fig. 7 shows that solution α_2 is nearly purely isovector for $R_c = 1.7$ and therefore may be ruled out. The allowed range for the isoscalar solution is $-\alpha_1 = 13.2$ to 2.6 for $R_c = 1.17$ to 2.27 .

We use both $\sigma_{\text{pk}}(\pi^+)$ and $\sigma_{\text{pk}}(\pi^-)$ to determine Z_1 . The Z_1 , α , and N correlations are shown in Fig. 8(b). Taking $N = 1.8 \pm 0.3$ and $-\alpha = 2.6$ to 13.2 , we can restrict $|Z_1|$ to the range 0.02 – 0.08 using both the π^- and the π^+ data. Thus we see that although the percentage error in determining Z_1 is large, the magnitude of Z_1 is determined to be quite small.

To get Z_0 and its error we use the more accurately measured π^+ cross section and use the equation

$$Z_0 = \frac{1}{a} \left\{ Z_1 \pm \left[\frac{\sigma(\pi^+)}{N\sigma_{\text{DW}}} \right]^{1/2} \right\}. \quad (12b)$$

Since Z_1 and Z_0 must have opposite sign, we require the plus sign for the second term on the right-hand side. Inserting $Z_1 = -(0.05 \pm 0.03)$, $\sigma_{\text{pk}}(\pi^+) = 33 \pm 4 \mu\text{b/sr}$, $\sigma_{\text{DW}} = 88.5 \mu\text{b/sr}$, $N = 1.8 \pm 0.3$, and $a = 1.93$, we obtain $Z_0 = 0.22 \pm 0.06$. The value of $-\alpha = 4.4$ corresponds to $R = 1.75$ by use of Eq. (10).

The determined values of Z_0 and Z_1 for all three of these 4^- states are given in the last columns of Table I. Comparison of these results to those in Table II of Ref. 7 for the 11.7- and 17.3-MeV states indicates that our answers fall within the range allowed by their analysis. Furthermore, it is clear that our pion cross-section data significantly narrow the allowed ranges for Z_0 and Z_1 , providing a more definitive test of wave functions predicted by nuclear structure calculations.

VI. PREDICTION OF $^{14}\text{C}(p,p')$ CROSS SECTIONS

Inelastic proton scattering can be used to confirm our determination of the Z coefficients for these 4^- states based on electron and pion-scattering data. We note that for unnatural-parity transitions 135-MeV protons see $\Delta T = 1/\Delta T = 0$ in amplitude ratio 1 to 1.3 at $q \approx 1.5 \text{ fm}^{-1}$, and thus are not as sensitive a probe of neutron-proton differences as pions. To estimate the usefulness of such a measurement, we performed standard distorted wave approximation (DWA) calculations for $^{14}\text{C}(p,p')$ at 135 MeV using the free t matrix given in Ref. 28, which gave good results for the stretched states in ^{28}Si and ^{24}Mg (Refs. 2 and 3). We used the ^{12}C optical potential of Ref. 29, which should be adequate for our purpose here. Calculations were performed using the code DWBA70.³⁰

The solid curves in Fig. 9 show the predictions based on the values of Z_0 and Z_1 given in Table I. The shaded area in Fig. 9 shows the range of proton cross sections allowed for the 11.7- and 17.3-MeV states if *only* the electron-scattering measurements⁷ and the limits on the π^+/π^- ratios⁶ R were known. We see that the more accurate determination of Z_0 using the absolute π^\pm cross sections considerably reduces the range of the predicted proton cross sections.

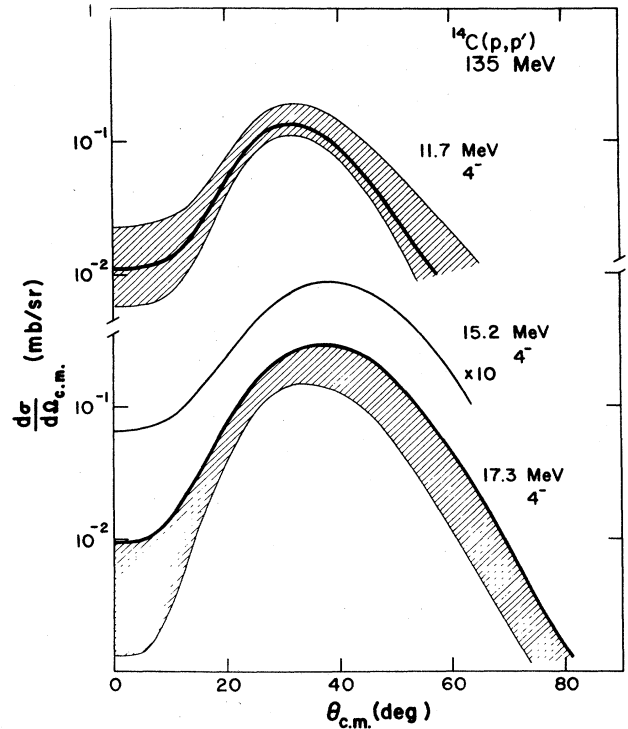


FIG. 9. Predicted proton cross sections for the 4^- states. The dark solid line is based on the Z coefficients deduced in this work (Table I). The shaded area represents the range of cross sections allowed by the Z coefficients obtained from electron scattering (Ref. 7) and the use of the limits on $R = \sigma(\pi^+)/\sigma(\pi^-)$ given in Ref. 6.

TABLE II. Parentage expansions of ¹⁴C states to common parents $JT\alpha$ of $A=13$ that are present in the expansion of the 0⁺ ground state. For negative-parity states the parent is coupled to a $d_{5/2}$ nucleon; for the 0⁺ ground state the coupling is to a $1p$ nucleon. Calculated excitation energies in MeV are given in the last row.

$JT\alpha$	4 ^{-a}	4 ^{-b}	4 ^{-c}	4 ^{-d}	3 ^{-a}	0 ⁺ a
$\frac{1}{2} \frac{1}{2} a$					-0.912	-0.409
$\frac{3}{2} \frac{1}{2} a$	-0.852	+0.436	+0.014	-0.081	+0.040	-0.445
$\frac{3}{2} \frac{1}{2} b$	+0.035	+0.044	+0.608	+0.569	+0.040	-0.138
$\frac{3}{2} \frac{3}{2} a$	+0.106	+0.163	-0.624	+0.324	+0.191	-0.675
E_x (MeV)	12.0	13.4	16.2	17.2	6.3	0

VII. SHELL-MODEL CALCULATIONS

A. Model space and eigenvalues

The negative-parity states were calculated in the space $(1p)^{-3}(2s,1d)$ with a slightly modified form of the Millener-Kurath³¹ interaction. In this space there are 29 states with $J^\pi=4^-$ starting at an excitation energy of about 12 MeV in ¹⁴C, and 53 states with $J^\pi=3^-$ starting at about 6-MeV excitation. The positive-parity states were calculated in the space $(1p)^{-2}+(1p)^{-4}(2s,1d_{5/2})^2$, where only neutrons are excited to the $(2s,1d)$ shell. This results in two strongly mixed $J^\pi=2^+$ states, as discussed in Refs. 6 and 15, and a $J^\pi=0^+$ ground state that is mainly $(1p)^{-2}$ with a 5%-intensity admixture of a state consisting of the ¹²C ground state coupled to two neutrons as in the ground state of ¹⁸O. In Table II there is a listing of parentage amplitudes for the lowest 0⁺ and 3⁻ states

and for the four lowest 4⁻ states of ¹⁴C to states of $A=13$, which are common parents to both the 0⁺ ground state and the negative-parity states. These are the components needed to calculate transition amplitudes from the ground state; the rest of the J^- parentage is mainly to the lowest $J=\frac{5}{2}$ and $\frac{7}{2}$ states with $T=\frac{1}{2}$. Calculated excitation energies are also listed. Since the ¹⁴C states in Table II all have $T=1$, the $T=\frac{1}{2}$ parentage will lead to neutron transitions from the ground state and consequently favor π^- excitation over π^+ excitation. Only the $J=4^-c$ state has large parentage to the lowest $T=\frac{3}{2}$ state, and hence favors π^+ excitation.

B. Peak cross sections

The peak cross sections for strong transitions can be obtained by the approximate formulas of Lee and Kurath²⁵ with parameters appropriate to ¹⁴C,

$$\frac{d\sigma}{d\Omega}(\pi^-, \theta_{pk}, JLS) = C_{JLS}(2J+1)\{3[A_{Jn}(d^\dagger p) - A_{Jn}(p^\dagger d)] + \rho_J A_{Jp}(d^\dagger p)\}^2, \quad (13a)$$

$$\frac{d\sigma}{d\Omega}(\pi^+, \theta_{pk}, JLS) = C_{JLS}(2J+1)\{\rho_J[A_{Jn}(d^\dagger p) - A_{Jn}(p^\dagger d)] + 3A_{Jp}(d^\dagger p)\}^2, \quad (13b)$$

with $C_{431}=4.7 \mu\text{b}$, $\rho_4=1$, $\theta_{pk}=64^\circ$ and $C_{330}=15.7 \mu\text{b}$, $\rho_3=1.13$, $\theta_{pk}=44^\circ$. The calculated transition-density amplitudes and the peak differential cross sections for the

four 4⁻ states and the lowest energy 3⁻ state are given in Table III. The amplitudes $A_{Jn}(p^\dagger d)$ (annihilation of a $d_{5/2}$ neutron and creation of a $p_{3/2}$ neutron) listed in the

TABLE III. Theoretical transition-density amplitudes for neutron (A_{Jn}) and proton (A_{Jp}) excitation of 4⁻ and 3⁻ states in ¹⁴C and the corresponding theoretical peak cross sections.

J_σ	$B(M4)^\dagger$ ($\mu_N^2 \text{ fm}^6$) (10 ³)	$A_{Jn}(d^\dagger p)$	$A_{Jn}(p^\dagger d)$	$A_{Jp}(d^\dagger p)$	$\sigma_{pk}(\pi^+)^a$ ($\mu\text{b}/\text{sr}$)	$\sigma_{pk}(\pi^-)^a$ ($\mu\text{b}/\text{sr}$)
4 ^{-a}	70	-0.581	-0.045	+0.077	4,4	98,113
4 ^{-b}	4	+0.351	+0.025	+0.116	19,23	50,57
4 ^{-c}	90	+0.034	+0.002	-0.480	84,105	6,7
4 ^{-d}	14	+0.078	+0.003	+0.253	29,35	10,11
3 ^{-a}		-0.668	+0.060	-0.177	201,172	624,516

^aValues on the left-hand side were obtained by Eq. (13); values on the right-hand side for 4⁻ states were obtained with distorted-wave calculations and normalizations discussed in Sec. IV. The amplitudes A_J given in this table were used. The values for the 3⁻ state on the right-hand side were calculated, as discussed in Sec. VII.

TABLE IV. Comparison of the experimental and theoretical proton and neutron spectroscopic amplitudes. These are related to experimental Z_0 and Z_1 given in Table I by $Z_n = (Z_0 + Z_1)/\sqrt{2}$ and $Z_p = (Z_0 - Z_1)/\sqrt{2}$. The theoretical values are obtained from Table III and the relations $Z_n = A_{Jn}(d^\dagger p) - A_{Jn}(p^\dagger d)$ and $Z_p = A_{Jp}(d^\dagger p)$ for the 4^- states.

E_x (MeV)	Experiment		E_x (MeV)	Theory	
	Z_p	Z_n		Z_p	Z_n
11.7	0.11±0.04	-0.36±0.04	12.0	0.08	-0.54
15.2	0.19±0.07	0.12±0.07	13.4	0.12	0.33
17.3	-0.37±0.03	0.01±0.03	16.2	-0.48	0.03

fourth column result from the $(1p)^{-4}(2s,1d)^2$ admixture in the ground state. They interfere constructively with the main amplitude for the 3^- state and destructively for the four 4^- states. The $B(M4)\uparrow$ values for relevant cross sections in inelastic electron scattering are given in the second column of Table III. The last two columns give the peak cross sections for π^+ and π^- scattering, the first number in each pair being the result of Eq. (13) and the second number being the result of the DWIA calculations described in Sec. IV. The absolute normalization of the predicted 4^- cross sections differ by about 15% between the two models.

In comparing the calculated cross sections for the 4^- states with the observed values (Table I), it is clear that the strong transitions to the 11.7- and 17.3-MeV states are qualitatively similar to the calculated transitions to 4^-a and 4^-c , respectively, since the lower state is strongly favored in π^- scattering, whereas the upper state is favored in π^+ scattering. The calculated cross sections for the 4^-b state do not agree with the observed values for the state at 15.2 MeV, considering that the calculated π^+/π^- ratio is the opposite of the observed value. The calculated peak cross sections for the lowest 3^- state are lower than the measured values. In this case it will be shown in the following that some isoscalar enhancement can lead to agreement with experiment.

Differences between the experimentally deduced wave functions and the theoretical wave functions for the 4^- states are more apparent by comparing the respective spectroscopic amplitudes. These amplitudes given in neutron-proton notation are shown in Table IV. Here it becomes clear that the theory tends to overestimate the neutron amplitudes Z_n . The proton amplitude Z_p is slightly underestimated for the 11.7-MeV state and slightly overestimated for the 17.3-MeV state (which is predicted at 16.2 MeV). Thus the structure calculations describe the fragmentation of the proton $M4$ strength, but must lack some essential physics required to get the fragmentation of the neutron-transition strength and the excitation energies correctly.

To test the effect of using more recent optical-potential parameters in the DWIA calculations than were employed in obtaining Eq. (13), we performed DWIA calculations for the 3^- state at 6.73 MeV using the code ARPIN.²⁵ The shell-model transition amplitudes were taken from the present work. The harmonic-oscillator parameter was

TABLE V. Sum-rule values calculated with a pure jj ground state, the Cohen-Kurath ground state, and a ground state including some neutrons in the $(2s,1d)$ shell. The final column gives the fraction going to 1p-1h states in the last case.

	$s^4p^{10}(jj)$	$s^4p^{10}(CK)$	Including $(sd)_n^2$	(1p-1h)
$S^4(p)$	1	0.929	0.923	0.880
$S^4(n)$	1	1.000	0.914	0.882
$S^{40}(1\rightarrow 1)$	1	0.965	0.919	0.881
$S^{41}(1\rightarrow 1)$	0.5	0.500	0.463	0.441
$S^{41}(1\rightarrow 2)$	0.5	0.465	0.456	0.440

chosen to be $b=1.63$ fm. The peak cross sections given by these calculations are 172 $\mu\text{b/sr}$ (π^+) and 516 $\mu\text{b/sr}$ (π^-) compared to 201 $\mu\text{b/sr}$ and 624 $\mu\text{b/sr}$, respectively, given by Eq. (13). We see that the use of different distortions generates peak cross sections that agree to 20% with those of Eq. (13).

The experimental peak cross sections, 490 ± 50 $\mu\text{b/sr}$ for π^+ and 1010 ± 80 $\mu\text{b/sr}$ for π^- , are larger than the theoretical cross sections, particularly for π^+ scattering. We can obtain good agreement with the peak cross sections by introducing polarization charges δ_n and δ_p to represent the fact that valence nucleons polarize the proton and neutron cores. A recent discussion for $E3$ transitions in pion scattering may be found in Refs. 32 and 33. The DWIA calculations shown in Figs. 4 and 5 were performed with enhancement factors $(1+\delta_p+\delta_n)=1.5$ for the isoscalar, spin-independent part of the transition density. No need was found for an isovector enhancement; that is, $(1+\delta_p-\delta_n)=1.0$ was used, so that $\delta_p=\delta_n=\delta=0.25$. This value of δ is smaller than the 0.6 obtained³² for the strongly collective 3^- transitions in ^{16}O and ^{17}O . The smaller value of δ for ^{14}C is consistent with the lower $B(E3)$ value for this state³⁴ as compared to $B(E3)$ values for the 3^- states ^{12}C (9.64 MeV) (Ref. 35) and ^{16}O (6.13 MeV) (Ref. 36).

VIII. SUM RULES FOR STRETCHED STATES

A. General expressions

The particle-hole operator for a stretched transition, $\lambda=j_1+j_2$, is

$$Q^\lambda(t_3) \equiv Q^{\lambda(j_2 j_1)}(t_3) - Q^{\lambda(j_1 j_2)}(t_3), \quad (14)$$

where

$$Q^{\lambda(jj')}(t_3) = (a_{t_3}^{j\dagger} \times \bar{a}_{t_3}^{j'})^\lambda$$

with $\bar{a}_m^j = (-1)^{j+m} a_{-m}^j$. Here a^\dagger and a are the usual creation and annihilation operators and t_3 indicates either a neutron (n) or a proton (p). One can write a sum rule in terms of the double-barred reduced-matrix elements (RME) from the Wigner-Eckart theorem

$$\begin{aligned} \langle \psi_M^{j\alpha} | Q_{\lambda_z}^\lambda(t_3) | \psi^{j_0\alpha_0} \rangle \\ = (J_0 \lambda M_0 \lambda_z | JM) \langle \psi^{j\alpha} | | Q^\lambda(t_3) | | \psi^{j_0\alpha_0} \rangle. \end{aligned} \quad (15)$$

The sum rule for transitions from the $J_0\alpha_0$ ground state to all excited states is

$$S^\lambda(t_3) = (\hat{J}_0\hat{\lambda})^{-1} \sum_{J\alpha} \hat{J} \langle \psi^{J_0\alpha_0} | Q^\lambda(t_3) | \psi^{J_0\alpha_0} \rangle^2, \quad (16a)$$

which by closure equals

$$S^\lambda(t_3) = (\hat{\lambda})^{-1} \left\langle \psi_{M_0}^{J_0\alpha_0} \left| \sum_{\lambda_z} Q_{\lambda_z}^{\lambda\dagger}(t_3) Q_{\lambda_z}^\lambda(t_3) \right| \psi_{M_0}^{J_0\alpha_0} \right\rangle. \quad (16b)$$

Here we define $\hat{J} \equiv 2J + 1$.

Alternatively, one can use the isospin-coupled form of the operator

$$Q_{\lambda_z}^{\lambda\tau} \equiv \frac{1}{\sqrt{2}} [Q^\lambda(n) + (-1)^\tau Q^\lambda(p)]. \quad (17)$$

The isospin form of the sum rules is then

$$S^{\lambda\tau} = \frac{1}{2} [S^\lambda(n) + S^\lambda(p)] + (-1)^\tau (\hat{\lambda})^{-1} \times \left\langle \psi_{M_0}^{J_0\alpha_0} \left| \sum_{\lambda_z} Q_{\lambda_z}^{\lambda\dagger}(n) Q_{\lambda_z}^\lambda(p) \right| \psi_{M_0}^{J_0\alpha_0} \right\rangle, \quad (18)$$

wherein the two cross terms are combined, since the operator sum is Hermitian.

There are no j_2t_3 nucleons in the ground state. In this case the second term of Q^λ in Eq. (14) does not contribute and the sum rules simply depend on the number of j_1t_3 nucleons in $(J_0T_0\alpha_0) \equiv (0)$. The sum rules become

$$S^\lambda(t_3) = (\hat{j}_1)^{-1} \langle n_{t_3}^{j_1} \rangle_0, \quad (19a)$$

$$S^{\lambda\tau} = \frac{1}{2} [S^\lambda(n) + S^\lambda(p)] = (2\hat{j}_1)^{-1} \langle n_n^{j_1} + n_p^{j_1} \rangle_0. \quad (19b)$$

The $Q(n)Q(p)$ cross term of Eq. (18) vanishes if there are no j_2t_3 nucleons in (0). The isovector sum rule can be split into transitions from the T_0 ground state to states with $T = T_0$ and to states with $T = T_0 + 1$,

$$S^{\lambda 1}(T_0 \rightarrow T_0 + 1) = (2\hat{j}_1)^{-1} \left\langle \frac{2}{T_0 + 1} n_p^{j_1} \right\rangle_0, \quad (20a)$$

$$S^{\lambda 1}(T_0 \rightarrow T_0) = (2\hat{j}_1)^{-1} \left\langle n_n^{j_1} + \left[\frac{T_0 - 1}{T_0 + 1} \right] n_p^{j_1} \right\rangle_0. \quad (20b)$$

This shows that as T_0 increases, the fraction of isovector transition strength going to $T_0 + 1$ states decreases.

There are j_2 nucleons present in the ground state. In this case the evaluation of Eq. (16b) and its isospin analog Eq. (18) requires a more complex expression,

$$\begin{aligned} \left\langle (\hat{\lambda})^{-1} \sum_{\lambda_z} Q_{\lambda_z}^{\lambda\dagger}(\bar{t}_3) Q_{\lambda_z}^\lambda(t_3) \right\rangle_0 &= \delta_{\bar{t}_3, t_3} \langle (\hat{j}_1)^{-1} n_{t_3}^{j_1} + (\hat{j}_2)^{-1} n_{t_3}^{j_2} \rangle_0 \\ &+ 2 \sum_K W(j_1 j_1 j_2 j_2; K \lambda) \left[2 \sum_{TT_3} (-1)^{T-1} \left(\frac{1}{2} \frac{1}{2} \bar{t}_3 t_3 \mid TT_3 \right)^2 \left\langle \sum_{K_z} C_{K_z T_3}^{KT(j_1^2)\dagger} C_{K_z T_3}^{KT(j_2^2)} \right\rangle_0 \right. \\ &\quad \left. - \left\langle \sum_{K_z} (-1)^{K-K_z} (a_{\bar{t}_3}^{j_1} \times \bar{a}_{t_3}^{j_1})_{K_z}^K (a_{t_3}^{j_2} \times \bar{a}_{\bar{t}_3}^{j_2})_{-K_z}^K \right\rangle_0 \right]. \quad (21) \end{aligned}$$

Here $C^{KT(j^2)\dagger}$ is a creation operator for two nucleons in the orbital j , which produces a normalized two-body wave function when applied to the vacuum; $K + T$ must be odd. The term W is a Racah coefficient. For Eq. (16b), $\bar{t}_3 = t_3$, the squared isospin Clebsch-Gordan (CG) coefficient is unity, $T = 1$, and $T_3 = 2t_3$. For the cross term of Eq. (18), $\bar{t}_3 = n$ and $t_3 = p$ so that $T_3 = 0$ and the squared CG coefficient is 0.5. The cross term contributes only when there are both neutrons and protons in the j_2 level. The sum rule for transitions to $T_0 + 1$ states becomes

$$\begin{aligned} (T_0 + 1) S^{\lambda 1}(T_0 \rightarrow T_0 + 1) &= \langle (\hat{j}_1)^{-1} n_p^{j_1} + (\hat{j}_2)^{-1} n_p^{j_2} \rangle_0 \\ &+ \sum_K W(j_1 j_1 j_2 j_2; K \lambda) \left[2 \sum_{K_z} \left\langle \sum_{K_z} C_{K_z 0}^{KT(j_1^2)\dagger} C_{K_z 0}^{KT(j_2^2)} \right\rangle_0 \right. \\ &\quad \left. - \sum_{t_3} \left\langle \sum_{K_z} (-1)^{K-K_z} (a_{-t_3}^{j_1} \times \bar{a}_{-t_3}^{j_1})_{K_z}^K (a_{t_3}^{j_2} \times a_{t_3}^{j_2})_{K_z}^K \right\rangle_0 \right]. \quad (22) \end{aligned}$$

In Eq. (22) the term with the C^{KT} product contributes only if both neutrons and protons are present in the j_2 level.

If there are only neutrons in the j_2 level, the physically most likely situation, there is no cross term in Eq. (18) and $S^\lambda(p)$ is given by Eq. (16b). If in addition the neutrons in j_2 are coupled to angular-momentum zero, only $K = 0$ terms occur in Eqs. (21) and (22), and since

$$(a_{t_3}^{j_1} \times \bar{a}_{t_3}^{j_1})^0 = -(\hat{j})^{1/2} n_{t_3}^{j_1},$$

we get the simpler forms

$$\begin{aligned} S^\lambda(n) &= (\hat{j}_1)^{-1} \langle n_n^{j_1} \rangle_0 + (\hat{j}_2)^{-1} \langle n_n^{j_2} \rangle_0 - 2(\hat{j}_1\hat{j}_2)^{-1} \langle n_n^{j_1} n_n^{j_2} \rangle_0 \\ &\quad + 4(\hat{j}_1\hat{j}_2)^{1/2} \langle C_{01}^{01(j_1^2)\dagger} C_{01}^{01(j_2^2)} \rangle_0. \quad (23) \end{aligned}$$

and

$$(T_0+1)S^{\lambda_1}(T_0 \rightarrow T_0+1) \\ = (\hat{j}_1)^{-1} \langle n_p^{j_1} \rangle_0 - (\hat{j}_1 \hat{j}_2)^{-1} \langle n_p^{j_1} n_n^{j_2} \rangle_0. \quad (24)$$

Two points should be kept in mind about these sum rules. If there are j_2 nucleons in the ground state, then in addition to making transitions to the level j_1 , they can also be excited to some higher level, j_3 , with multipolarity λ . This possibility has been ignored in obtaining the sum rules, since it is not likely to make a noticeable condition in physically realized situations. A second point is that the calculated sum includes contributions from transitions to states of spurious center-of-mass excitation. This contribution can be calculated, and it is a few percent effect for stretched transitions.

B. Results for ^{14}C

In the case of ^{14}C the stretched 4^- transition arises from $j_1 = p_{3/2}$ and $j_2 = d_{5/2}$. Three models of the ground state are considered in order to show the effect on the sum rules. The simplest is the jj limit, wherein the $p_{3/2}$ shell is full for both neutrons and protons. Next is the ground state for the Cohen-Kurath (8-16)2B interaction,³⁷ which has $n_p^{p_3} = 4(0.929)$. Finally, we consider a ground state containing some neutrons in the $(2s, 1d)$ shell. A good approximation to the result of a shell-model calculation is

$$\psi^{01}(^{14}\text{C}) = (1 - \beta_1^2 - \beta_5^2)^{1/2} \phi^{01a}(^{14}\text{C}) \\ + \phi^{00a}(^{12}\text{C}) \times [\beta_1 C^{01\dagger(2s^2)_n} + \beta_5 C^{01\dagger(d^2)_n}], \quad (25)$$

with $\beta_1 = -0.106$ and $\beta_5 = -0.203$. The two ϕ 's are pure $1p$ -shell ground-state wave functions for ^{14}C and ^{12}C . In this approximation only the $K=0$ terms contribute and we use Eqs. (23) and (24). The sum rules for ^{14}C are

$$S^4(p) = (4)^{-1} \langle n_p^{p_3} \rangle_{01}, \quad (26)$$

for the protons and

$$S^4(n) = [(4)^{-1} \langle n_n^{p_3} \rangle_{01} + (6)^{-1} \langle n_n^{d_5} \rangle_{01} - (12)^{-1} \langle n_n^{p_3} n_n^{d_5} \rangle_{01} \\ + 2(6)^{-1/2} \langle C_{01}^{01(p_3^2)\dagger} C_{01}^{01(d_5^2)} \rangle_{01}] \quad (27)$$

for the neutrons. For the $T_0=1$ to $T=2$ transitions, one has

$$S^{41}(1 \rightarrow 2) = (8)^{-1} \langle n_p^{p_3} \rangle_{01} - (48)^{-1} \langle n_p^{p_3} n_n^{d_5} \rangle_{01}. \quad (28)$$

In order to evaluate the expectation values with the wave function of Eq. (25), we use the calculated value of the number of $p_{3/2}$ protons (or neutrons) in the ^{12}C ground state, $\langle n_{i_3}^{p_3} \rangle_{00a} = 3.298$; and in order to evaluate the last expectation value in $S(n)$, we also need the matrix element

$$\langle \phi^{01a}(^{14}\text{C} | C_{01}^{01(p_3^2)\dagger} | \phi^{00a}(^{12}\text{C}) \rangle = 0.417.$$

Numerical values for the three models are given in Table V. One sees that the presence of $(2s, 1d)$ neutrons produces an appreciable decrease in the sum-rule values,

considering that it is only a 5% admixture in the wave function. The last column of Table V gives the amount of the sum rule going to $1p$ - $1h$ states. The remainder goes to $3p$ - $3h$ states that arise when the Q^4 operator excites a $p_{3/2}$ nucleon from the ^{12}C ground state into a $d_{5/2}$ level.

IX. DISCUSSION

Comparison of the neutron and proton spectroscopic amplitudes deduced from the data with those given by the shell-model calculations (Table IV) shows that the structure calculations considerably overestimate the neutron contribution in all three 4^- states. The proton contribution is underestimated for the 11.7- and 15.2-MeV states and slightly overestimated for the 17.3-MeV state.

We can also compare the experimental sum-rule strengths with the shell-model values given in Table V. For the $T=1$ states at 11.7, 15.2, and 17.3 MeV, the experimental values are

$$S^{40}(1 \rightarrow 1) = \Sigma Z_0^2 = 0.15 \pm 0.08$$

and

$$S^{41}(1 \rightarrow 1) = \Sigma Z_1^2(T=1) = 0.19 \pm 0.03.$$

For the $T=2$ state at 24.3 MeV, the $^{14}\text{C}(e, e')$ experiment yielded⁷ $Z_1 = 0.40 \pm 0.04$, which gives $S^{41}(1 \rightarrow 2) = 0.16$. The observed value of S^{40} represents only 16% of the theoretical value and the observed $S^{41}(1 \rightarrow 1)$ and $S^{41}(1 \rightarrow 2)$ strengths represent 41% and 35% of the calculated values, respectively.

Apparently the $1p$ - $1h$ space used in the calculation of the negative-parity states is insufficient. Earlier weak-coupling calculations of Lie³⁸ included $3p$ - $3h$ states constructed by coupling the $J^\pi = \frac{3}{2}^-, T = \frac{1}{2}$ ground state of $A=11$ to the lowest $T = \frac{1}{2}$ states with a $(2s, 1d)^3$ configuration, such as $J = \frac{3}{2}^+$. Lie obtained a $4^-, T=0$ state of this type within 5 MeV of his lowest $4^-, T=0$ state. Thus one might also expect a $4^-, T=1$ state with the same structure within 5 MeV of the lowest $4^-, T=1$ state. The mixing of such states with the $1p$ - $1h$ states will result in some energy shift and redistribution of the single-particle transition strength from the ground state. Such a $3p$ - $3h$ configuration can only be reached by proton excitation from the $2p$ - $2h$ component of our ground state. This might offer an explanation for the observed cross sections.

There is some evidence for appreciable $3p$ - $3h$ components in the 11.7- and 15.2-MeV states from recent investigations³⁹ of the three-particle transfer reactions $^{11}\text{B}(^6\text{Li}, ^3\text{He})^{14}\text{C}$ and $^{11}\text{B}(^7\text{Li}, \alpha)^{14}\text{C}$. In the 10° spectrum of the $(^6\text{Li}, ^3\text{He})$ reaction, which corresponds to an angular-momentum mismatch of approximately $4\hbar$, large peaks are seen at 11.73 and 15.19 MeV and a small peak is at 17.28 MeV. These three states appear to correspond to the 4^- states that we have identified at 11.7, 15.2, and 17.3 MeV. If this is indeed the case, it constitutes evidence for the existence of appreciable $3p$ - $3h$ components in the lower two states and much smaller such components in the 17.3-MeV state.

The $(^6\text{Li}, ^3\text{He})$ and $(^7\text{Li}, \alpha)$ data³⁹ show that there are two states at 11.67 and 11.73 MeV, with the latter having

properties expected for a 4^- state and the former appearing to be a low-spin state. The lower spin state may be showing up in the low-momentum transfer (30°) part of the angular distribution shown in Fig. 2. Clearly, $^{14}\text{C}(p,p')$ measurements would be useful in clarifying the level structure in this excitation region.

X. CONCLUSIONS

We used the clear signature for identifying $M4$ excitations in pion-scattering excitation functions and differential cross sections to identify three new 4^- states in ^{14}C , two of which have been confirmed by 180° electron scattering. Pion differential cross sections and $\sigma(\pi^+)/\sigma(\pi^-)$ ratios show an enhanced sensitivity to the isoscalar component of spin transitions that is complemented by the sensitivity of magnetic electron scattering to isovector components. For stretched states, this combination of data permits the accurate determination of the particle-hole transition amplitudes Z_0 and Z_1 within the uncertainties of DWA in calculations for pion-inelastic scattering to unnatural-parity states.

The deduced amplitudes were compared to shell-model predictions of the distribution of $M4$ strength. The two states at 11.7 and 17.3 MeV are described well, although a deficiency exists in the neutron components of the

theoretical wave function. Overall about 40–50% of the expected isovector strength (S^{41}) was observed, whereas only about 16% of the expected isoscalar strength (S^{40}) was seen. This quenching is similar to what has been observed for other stretched states.^{1–3,17,27} It appears that 3p-3h configurations may be required to obtain the observed excitation energies and wave functions. Recent results from three-particle transfer experiments indicate that such components are present in several of the 4^- states discussed. It is clear that stretched states, which are primarily excited via a single isospin-dependent density, provide a stringent test of the fragmentation and distribution $M4$ strength predicted by nuclear structure calculations for p -shell nuclei. Understanding the $M4$ strength distribution should contribute to a better theoretical understanding of the quenching of other spin-flip transitions in light nuclei.

ACKNOWLEDGMENTS

The authors are indebted to Dr. T.-S. H. Lee for making his computer code ARPIN available to us and for valuable discussion regarding its use. We also thank M. C. L. Blilie for doing some of the DWIA calculations. One of us (J.A.C.) wishes to thank F. Petrovich for useful discussions.

*Present address: Los Alamos National Laboratory, Los Alamos, NM 87545.

¹F. Petrovich and W. G. Love, Nucl. Phys. **A354**, 499c (1981).

²F. Petrovich, W. G. Love, A. Picklesimer, G. E. Walker, and E. R. Siciliano, Phys. Lett. **95B**, 166 (1980).

³R. A. Lindgren, W. J. Gerace, A. D. Bacher, W. G. Love, and F. Petrovich, Phys. Rev. Lett. **42**, 1524 (1979).

⁴S. J. Seestrom-Morris, D. Dehnhard, D. B. Holtkamp, and C. L. Morris, Phys. Rev. Lett. **46**, 1447 (1981).

⁵E. R. Siciliano and G. E. Walker, Phys. Rev. C **23**, 2661 (1981).

⁶D. B. Holtkamp, S. J. Seestrom-Morris, S. Chakravarti, D. Dehnhard, H. W. Baer, C. L. Morris, S. J. Greene, and C. J. Harvey, Phys. Rev. Lett. **47**, 216 (1981).

⁷M. A. Plum, R. A. Lindgren, J. Dubach, R. S. Hicks, R. L. Huffman, B. Parker, G. A. Peterson, J. Alster, J. Lichtenstadt, M. A. Moinester, and H. W. Baer, Phys. Rev. Lett. **137B**, 15 (1984).

⁸H. A. Thiessen and S. Sobotka, Los Alamos National Laboratory Report LA-4534-MS, 1970 (unpublished).

⁹F. Petrovich, R. H. Howell, C. H. Poppe, S. M. Austin, and G. M. Crawley, Nucl. Phys. **A383**, 355 (1982).

¹⁰Carol J. Harvey, Ph.D. thesis, University of Texas, 1984 (unpublished).

¹¹C. L. Morris, J. Piffaretti, H. A. Thiessen, W. B. Cottingham, W. J. Braithwaite, R. J. Joseph, I. B. Moore, D. B. Holtkamp, C. J. Harvey, S. J. Greene, C. F. Moore, R. L. Boudrie, and R. J. Peterson, Phys. Lett. **86B**, 31 (1979).

¹²S. J. Seestrom-Morris, D. Dehnhard, M. A. Franey, G. S. Kyle, C. L. Morris, R. L. Boudrie, J. Piffaretti, and H. A. Thiessen, Phys. C **26**, 594 (1982); S. J. Seestrom-Morris, D. Dehnhard, M. A. Franey, C. L. Morris, R. L. Boudrie, and H. A. Thiessen, *ibid.* **28**, 1301 (1983).

¹³D. Dehnhard, S. J. Tripp, M. A. Franey, G. S. Kyle, C. L. Morris, R. L. Boudrie, J. Piffaretti, and H. A. Thiessen, Phys. Rev. Lett. **43**, 1091 (1979).

¹⁴D. B. Holtkamp, W. J. Braithwaite, W. Cottingham, S. J. Greene, R. J. Joseph, C. F. Moore, C. L. Morris, J. Piffaretti, E. R. Siciliano, H. A. Thiessen, and D. Dehnhard, Phys. Rev. Lett. **45**, 420 (1980).

¹⁵D. Dehnhard, in Proceedings of the Ninth International Conference on High Energy Physics and Nuclear Structure, 1981, Versailles, France, Nucl. Phys. **A374**, 377c (1982).

¹⁶H. W. Baer, J. A. Bistirlich, K. M. Crowe, W. Dahme, C. Joseph, J. P. Pernoud, M. Lebrun, C. J. Martoff, U. Straumann, and P. Truöl, Phys. Rev. C **28**, 761 (1983).

¹⁷J. A. Carr, F. Petrovich, D. Halderson, D. B. Holtkamp, and W. B. Cottingham, Phys. Rev. C **27**, 1636 (1983).

¹⁸C. Olmer, B. Zeidman, D. F. Geesaman, T.-S. H. Lee, R. E. Segel, L. W. Swenson, R. L. Boudrie, G. S. Blanpied, H. A. Thiessen, C. L. Morris, and R. E. Anderson, Phys. Rev. Lett. **43**, 612 (1979).

¹⁹H. K. Lee and H. McManus, Nucl. Phys. **A167**, 257 (1971).

²⁰G. Rowe, M. Salomon, and R. H. Landau, Phys. Rev. C **18**, 584 (1978).

²¹F. Petrovich, Nucl. Phys. **A251**, 143 (1975).

²²D. S. Koltun, *Advances in Physics*, edited by M. Baranger and E. Vogt (Plenum, New York, 1969), Vol. 3, p. 71; G. A. Miller and J. E. Spencer, Ann. Phys. (N.Y.) **100**, 562 (1976).

²³J. A. Carr, F. Petrovich, D. Halderson, and J. J. Kelly, code ALLWORLD (unpublished).

²⁴J. A. Carr, code MSUDWPI (unpublished), adapted from the code DWPI, R. A. Eisenstein and G. A. Miller, Comput. Phys. Commun. **11**, 95 (1976).

²⁵T.-S. H. Lee and D. Kurath, Phys. Rev. C **24**, 1670 (1980).

- ²⁶L. J. Tassie and F. C. Barker, *Phys. Rev.* **111**, 940 (1958).
- ²⁷D. F. Geesaman (private communication), reanalysis of results in D. F. Geesaman *et al.*, *Phys. Rev. C* **27**, 1134 (1983) based on data from J. C. Bergstrom, R. Neuhausen, and G. Lahm, *Phys. Rev. C* **29**, 1168 (1984).
- ²⁸W. G. Love, A. Scott, F. Todd Baker, W. P. Jones, and J. D. Wiggins, Jr., *Phys. Lett.* **73B**, 277 (1978); W. G. Love, in *The (p,n) Reaction and the Nucleon-Nucleon Force*, edited by C. D. Goodman *et al.* (Plenum, New York, 1980), p. 23.
- ²⁹J. R. Comfort and B. C. Karp, *Phys. Rev. C* **21**, 2162 (1980); **22**, 1809(E) (1980).
- ³⁰J. Raynal and R. Schaeffer, computer code DWBA70 as modified by W. G. Love (unpublished).
- ³¹D. J. Millener and D. Kurath, *Nucl. Phys.* **A255**, 315 (1975).
- ³²D. Dehnhard and S. J. Seestrom-Morris, in *Proceedings of the International Symposium of Electromagnetic Properties of Atomic Nuclei, Tokyo, 1983*, edited by H. Horie and H. Ohnuma (Tokyo Institute of Technology, Tokyo, 1984), p. 225.
- ³³C. L. Blilie, D. Dehnhard, M. A. Franey, D. H. Gay, D. B. Holtkamp, S. J. Seestrom-Morris, P. J. Ellis, C. L. Morris, and D. J. Millener, *Phys. Rev. C* **30**, 1989 (1984).
- ³⁴F. Ajzenberg-Selove, *Nucl. Phys.* **A268**, 1 (1976).
- ³⁵F. Ajzenberg-Selove and C. L. Busch, *Nucl. Phys.* **A336**, 1 (1980).
- ³⁶F. Ajzenberg-Selove, *Nucl. Phys.* **A375**, 1 (1980).
- ³⁷S. Cohen and D. Kurath, *Nucl. Phys.* **73**, 1 (1965).
- ³⁸S. Lie, *Nucl. Phys.* **A181**, 517 (1972).
- ³⁹M. E. Clark and K. W. Kemper, *Nucl. Phys.* **A425**, 185 (1984).